ORIGINAL RESEARCH

On the Influence of the Extent of Oxidation on the Kinetics of the Hydrogen Electrode Reactions on Polycrystalline Nickel

Alexandr G. Oshchepkov[1] (ID) · **Antoine Bonnefont**[2] · **Elena R. Savinova**[3]
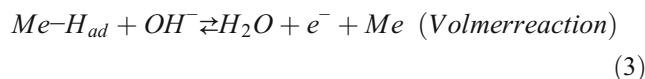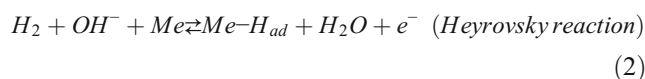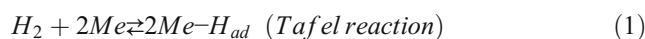
Abstract

The influence of the extent of oxidation of Ni electrodes on the kinetics of the hydrogen oxidation (HOR) and evolution (HER) reactions has been explored by combining an experimental cyclic voltammetry and chronoamperometry study with microkinetic modeling. The HOR/HER specific activity of the Ni/NiO$_x$ electrodes follows a volcano-type dependence with a maximum at 30% NiO$_x$ coverage corresponding to a 14-fold increase (nominally from 2.2 to 32.8 μA cm$^{-2}_{Ni}$) of the specific activity calculated as the exchange current density normalized by the electrochemical surface area of Ni active sites. The kinetic model suggests that the experimentally observed changes in the shape of current-potential curves as well as the HOR/HER specific activities are mostly due to the NiO$_x$ coverage–dependent strength of adsorption of hydrogen atoms. The latter is accompanied by an increase of the rate of the Volmer step and a decrease of the potential of OH$_{ad}$ adsorption on Ni centers in the vicinity of surface Ni oxides.

Keywords Nickel · Nickel oxide · Hydrogen oxidation reaction (HOR) · Hydrogen evolution reaction (HER) · Kinetic modeling · Alkaline media

Introduction

Alkaline hydrogen oxidation (HOR) and evolution (HER) reactions are among the most frequently studied processes because of their high importance for the development of alkaline exchange membrane fuel cells (AEMFCs) and water electrolyzers (AEMWEs). Besides they are ideal model reactions in electrocatalysis with an adsorbed H$_{ad}$ being the only reaction intermediate. The mechanism of the reactions includes the Volmer, Heyrovsky, and Tafel steps, which in alkaline media can be written as follows:

$$H_2 + 2Me \rightleftarrows 2Me-H_{ad} \quad (Tafel\ reaction) \tag{1}$$

$$H_2 + OH^- + Me \rightleftarrows Me-H_{ad} + H_2O + e^- \quad (Heyrovsky\ reaction) \tag{2}$$

$$Me-H_{ad} + OH^- \rightleftarrows H_2O + e^- + Me \quad (Volmer\ reaction) \tag{3}$$

Among non-noble metals, nickel is currently considered as the most promising electrocatalyst for the HOR/HER, demonstrating relatively high activity while being a low cost metal and possessing high corrosion stability in alkaline electrolytes [1–4]. It has been shown that the activity of Ni in the HOR/HER can be significantly enhanced when combined with Cu, Mo, Cr, or nitrogen [5–13]. Among non-noble electrodes, these materials are currently showing the best performance in AEMFCs and in AEMWEs likely due to an electronic effect of the second element. Besides, even without addition of another metal, the specific activity of Ni itself can be dramatically (more than 10 times) enhanced by precisely controlling the composition of the Ni surface [14–17]. To allow high activity in the HOR/HER, the latter must consist of both

✉ Alexandr G. Oshchepkov
oshchepkov@catalysis.ru

1 Boreskov Institute of Catalysis, Lavrentiev Ave. 5, Novosibirsk, Russia 630090

2 Institut de Chimie de Strasbourg, UMR 7177 CNR, University of Strasbourg, 4 rue Blaise Pascal, 67070 Strasbourg, France

3 Institut de Chimie et Procédés pour l'Energie, l'Environnement et la Santé, UMR 7515 CNRS, University of Strasbourg, 25 rue Becquerel, 67087 Strasbourg Cedex, France

metallic (Ni^0) and oxidized (NiO_x) sites. Note that adsorption of the H_{ad} intermediate takes place only on the metallic Ni centers [18], while the role of NiO_x species is still debated. Two hypotheses have been put forward. The first suggests that Ni surface oxides decrease the strength of H_{ad} adsorption on the nearby Ni^0 sites (which is otherwise too high on pure metal Ni electrode) [14, 19, 20]. The second hypothesis assumes that Ni surface oxides affect H_2O dissociation providing OH_{ad} and H_{ad} species for a bifunctional HOR/HER mechanism [16, 21]. Note that electrodeposited Ni/C nanoparticles with an optimized Ni/NiO_x surface state are currently state-of-the-art platinum-group metal-free electrocatalysts for the HOR/HER in alkaline media in terms of both specific and mass activity [15]. Theoretical calculations performed recently by Dong et al. have shown that the Gibbs free energy of H_{ad} adsorption ($\Delta_{ad}G_H^0$) on Ni varies depending on the quantity of closely located O(H) species, the latter correlating with the estimated exchange current density in the HER which reaches a maximum at 3/8 surface coverage by oxygen [22]. Pan et al. have experimentally demonstrated that the activity of Ni/C nanoparticles in the HOR depends on the amount of generated $Ni(OH)_2$ species on their surface with a maximum value (in terms of the total current) obtained for $Ni(OH)_2$:Ni surface molar ratio close to 1.1:1 [23]. However, comparison of the absolute values of the HOR currents is somewhat confusing and leaves the question about variation of the intrinsic activity of partially oxidized Ni samples open. Besides, it is not clear whether the $\Delta_{ad}G_H^0$ value is NiO_x coverage dependent, and whether it is the only reason for the changes in the HOR/HER activity of the Ni/NiO_x electrodes.

In the present work, we analyze the influence of the surface coverage of a bulk Ni electrode by NiO_x species on its activity in the HOR/HER at low overpotentials. The use of a bulk polycrystalline Ni electrode allows one to obtain reproducible initial surface state after polishing and thus ensure precise determination of the intrinsic electrocatalytic activity of the Ni/NiO_x electrodes in the HOR/HER depending on the extent of their oxidation. In comparison with the previous studies where the effect of NiO_x species on the HOR/HER kinetics of Ni has been discussed, this work for the first time compares *specific activities* of Ni/NiO_x electrodes with various surface coverage of NiO_x species. By performing microkinetic modeling, we analyze the influence of the NiO_x coverage on the kinetics of the Heyrovsky and Volmer steps as well as the adsorption of OH_{ad} species on Ni sites.

Experimental and Modeling Details

Materials

For electrochemical experiments, all solutions were prepared using ultrapure water produced by Mili-Q (Millipore, USA)

apparatus (18.2 MΩ cm, TOC < 5 ppb) and NaOH (50% in water, Premium quality, Aldrich). High-purity gases (Ar 99.998% and H_2 99.99%) were used for the measurements.

Electrochemical Measurements

The working electrode was a polycrystalline Ni rod (Ø5 mm, Mateck, 99.99%) fixed in a Teflon holder and sealed with the Teflon tape so that only the flat top surface of the electrode was accessible to the electrolyte. Prior to each experiment, the top surface of the Ni rod was thoroughly polished with an Al_2O_3 slurry (0.3 μm, Alfa Aesar) and rinsed by H_2O. Short polishing time and utilization of the Al_2O_3 granules with 0.3-μm size (and not 0.05 μm) while not allowing to obtain a smooth surface (the roughness factor was typically around 3) were preferred since they allowed to fully renew the Ni surface (i.e., to remove Ni oxides from the surface) and thus achieve high reproducibility of the measurements.

Electrochemical measurements were performed in a three-electrode glass cell thermostated at 25 °C using an Autolab PGSTAT 30 potentiostat (EcoChemie) equipped with a Scangen module. The counter electrode (Pt foil) and the reference electrode (Hg|HgO|0.10 M NaOH) separated compartments were connected with the working electrode chamber via a glass frit and a Luggin capillary, respectively. All electrode potentials reported in the manuscript are referred to the reversible hydrogen electrode (RHE, $E_{Hg/HgO/0.10\ M\ NaOH}$ = 0.928 V vs RHE). Prior to each experiment, the glassware was cleaned by soaking in a H_2SO_4:H_2O_2 (1:1 v/v) mixture and then thoroughly washed with ultrapure water.

Electrochemical measurements of Ni electrodes were performed right after polishing to avoid (as much as possible) surface passivation by oxygen from air. After immersion in Ar-saturated 0.10 M NaOH, the electrodes were cycled 3 times between − 0.20 and 0.40 V at a sweep rate (v) 20 mV s^{-1} in order to remove oxide species formed on their surfaces during the transfer to the cell. After that the Ni electrodes were conditioned by cycling between − 0.06 and 0.40 V at v = 20 mV s^{-1} until stabilization of the cyclic voltammetry (CV) profiles (with registering typically 3 scans). The latter CVs were analyzed for estimation of the electrochemical surface area (ECSA, S_{Ni}) of Ni considering the entire value of the anodic charge and the 0.514 mC cm^{-2} conversion coefficient. In order to study the influence of the surface state of Ni on its activity in the HOR/HER, the electrode was subjected to electrochemical oxidation detailed in Table 1, followed by partial reduction of the Ni surface by cycling between − 0.20 and 0.40 V at v = 20 and 5 mV s^{-1}. The amount of irreversible NiO_x species left on the electrode surface after such treatment is supposed to be constant between − 0.20 and 0.40 V. The ECSA of the resulting Ni/NiO_x electrodes ($S_{Ni/NiOx}$) was estimated from CVs recorded between − 0.06 and 0.40 V at v = 20 mV s^{-1}. Since the anodic charge corresponds to the amount

Table 1 Pretreatment procedure (by applying either cyclic voltammetry (CV) or chronoamperometry (CA)) used to obtain Ni electrodes with different NiO_x coverage and corresponding values of the apparent Tafel slope in the HER determined (with accuracy of ± 1 mV/decade) in the potential interval of $-0.20 < \eta < -0.07$ V

Sample	Pretreatment	θ_{NiOx}, %	Tafel slope, mV/decade
1	No	0	117
2	CV between − 0.3 and 1.0 V at v = 50 mV s^{-1} (1 scan)	6.5	122
3	CA at E = 1.0 V for t = 60 s	15.3	132
4	CA at E = 1.1 V for t = 120 s	29.1	142
5	CA at E = 1.2 V for t = 120 s	34.0	140
6	CA at E = 1.3 V for t = 300 s	42.1	135

of the metal Ni sites on the electrode surface, the oxide coverage can be estimated as follows:

$$\theta_{NiO_x} = \left(1 - \frac{S_{Ni/NiO_x}}{S_{Ni}}\right) \times 100\% \tag{4}$$

The example of such calculation is presented in the Supporting Information on Figure S1. The HOR/HER exchange currents were derived from the anodic scans of linear-sweep voltammograms obtained in H_2-saturated 0.10 M NaOH at v = 5 mV s^{-1} in the potential interval between − 0.20 (or − 0.06) and 0.40 V by linearization of the micropolarization region (from − 10 to 10 mV). Tafel analysis of the HER branches of CVs obtained at v = 5 mV s^{-1} was performed in the overpotential interval of $-0.20 < \eta < -0.07$ V.

Equations for the HOR/HER Kinetic Modeling on Ni

Mean-field microkinetic modeling of the HOR/HER current-potential curves was performed considering Volmer-Heyrovsky mechanism for the HOR/HER in alkaline media (Eqs. 2 and 3).

Although addition of the Tafel step allows one to better describe the HOR/HER kinetics close to the equilibrium potential, the exact contribution of this step compared with the Heyrovsky step cannot be unambiguously determined [19]. Therefore, it was disregarded in order to minimize the number of adjustable parameters. In addition, a proper description of the HOR/HER on Ni requires consideration of the Ni surface hydroxide formation and reduction, since it occurs in the same potential range as the HOR/HER processes. For this purpose, a two-step Ni-$(OH)_{2,ad}$ formation process was considered:

$$OH^- + Ni \rightleftarrows Ni - OH_{ad} + e^- \tag{5}$$

$$Ni - OH_{ad} + OH^- \rightleftarrows Ni - (OH)_{2,ad} + e^- \tag{6}$$
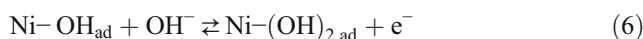
The coexistence of both Ni-H_{ad} and Ni-OH_{ad} species in the same potential interval might result in their recombination with the formation of water through the so called bifunctional mechanism [21].

$$Ni - H_{ad} + Ni - OH_{ad} \rightleftarrows H_2O + 2 Ni \tag{7}$$
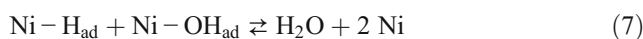
However, the contribution of the recombination step is rather unlikely on pure metallic Ni surface, because of the strong adsorption of H_{ad} on Ni and the high activation energy barrier for the reaction [24]. The reaction between H_{ad} and OH_{ad} becomes feasible when their adsorption energies are weakened ($\Delta_{ad}G_H^0$ of adsorption close to 0 eV), although its contribution cannot be unambiguously distinguished in this case from the one of the Volmer step in the microkinetic modeling. Besides, experimental results suggest a rapid blocking of the Ni surface by Ni-OH_{ad} species above 0.05 V [14, 19, 24]. Considering this, we will first perform kinetic modeling disregarding the recombination step and then show how its inclusion in the model affects the simulated current-potential curves.

The rates for the elementary steps of the HOR/HER as well as Ni-OH_{ad} and Ni-$(OH)_{2,ad}$ formation/reduction can be expressed as:

$$v_{H,i} = k_{H,i}^0 \left[\exp\left(\frac{(1-\alpha)F(E-E_{H,i})}{RT}\right) C_{H_2} C_{OH^-} \left(1 - \theta_H - \theta_{OH} - \theta_{(OH)_2}\right) - \exp\left(\frac{-\alpha F(E-E_{H,i})}{RT}\right) \theta_H \right] \tag{8}$$

$$v_{V,i} = k_{V,i}^0 \left[\exp\left(\frac{(1-\alpha)F(E-E_{V,i})}{RT}\right) C_{OH^-} \theta_H - \exp\left(\frac{-\alpha F(E-E_{V,i})}{RT}\right) \left(1 - \theta_H - \theta_{OH} - \theta_{(OH)_2}\right) \right] \tag{9}$$

$$v_{OH,i} = k_{OH,i}^0 \left[\exp\left(\frac{(1-\alpha)F(E-E_{OH,i})}{RT}\right) C_{OH^-} \left(1 - \theta_H - \theta_{OH} - \theta_{(OH)_2}\right) - \exp\left(\frac{-\alpha F(E-E_{OH,i})}{RT}\right) \theta_{OH} \right] \tag{10}$$

$$v_{(OH)_2,i} = k_{(OH)_2,i}^0 \left[\exp\left(\frac{(1-\alpha)F(E-E_{(OH)_2,i})}{RT}\right) C_{OH^-} \theta_{OH} - \exp\left(\frac{-\alpha F(E-E_{(OH)_2,i})}{RT}\right) \theta_{(OH)_2} \right] \tag{11}$$

The total Faradaic current density is then given by:

$$j_F = F \sum_{i=a_1,a_2} \theta_i \left(\upsilon_{H,i} + \upsilon_{V,i} + \upsilon_{OH,i} + \upsilon_{(OH)_2,i} \right) \quad (12)$$

Here, C_{H2} and C_{OH^-} are the concentrations of H_2 ($7 \cdot 10^{-4}$ M) and OH^- (0.1 M) in the solution divided by the standard concentration $C^\circ = 1$ M. Considering the fact that HOR on polycrystalline Ni occurs in the kinetic regime [25], these concentrations are assumed to be the same in the bulk of the electrolyte and near the electrode surface. θ_H, θ_{OH}, $\theta_{(OH)2}$ denote the surface coverage of the active intermediate Ni-H_{ad}, Ni-OH_{ad}, and Ni-$(OH)_{2,ad}$, respectively. Subscript i stands for the type of surface sites (for details see the "Kinetics of the HOR/HER and its Dependence on the Degree of Ni Oxidation" section). θ_i corresponds to the number of Ni active sites associated with either a_1 or a_2 anodic peaks (see "Kinetics of the HOR/HER and its Dependence on the Degree of Ni Oxidation" section for further details). In a first approximation, the diffusion coupling of these sites is neglected. k_V^0, k_H^0, k_{OH}^0, $k_{(OH)2}^0$ and E_V, E_H, E_{OH}, $E_{(OH)2}$ are the rate constants and standard potentials for the Volmer and Heyrovsky reactions and the formation/reduction of Ni-OH_{ad} and Ni-$(OH)_{2,ad}$, respectively. Langmuir adsorption isotherms were used with the aim to reduce the number of adjustable parameters, being in agreement with the previous studies [26, 27]. A Butler-Volmer dependence on the electrode potential E is assumed for the rate constants of the Heyrovsky and Volmer steps, where $\alpha = 0.5$ is the charge transfer coefficients and F, R, T are the Faraday constant, the ideal gas constant, and the temperature, respectively.

The value of $\Delta_{ad}G_H^0$, reffered to the RHE energy scale, can be expressed as following:

$$\Delta_{ad}G_H^0 = -FE_{V,i} \quad (13)$$

To account for the HOR/HER equilibrium potential at 0 V vs RHE in the simulated current-potential curves, the relation between the equilibrium potentials (vs RHE) of Heyrovsky and Volmer reaction steps has to obey the following equation:

$$E_{H,i} = -E_{V,i} + \frac{RT}{F} \ln C_{H_2} \quad (14)$$

A detailed description of the kinetic model can be found in our previous publications [14, 19]. It has been shown [14, 19] that the developed model could reproduce the shape of experimental current-potential curves for metallic and for partially oxidized Ni electrodes. The main experimental features observed for a partially oxidized Ni electrode could be captured by the kinetic model assuming a decrease of the adsorption energy of the hydrogen intermediate along with an increase of the rate constant of the Volmer step in the presence of surface NiO_x.

The main purpose of this work is to study the effect of NiO_x surface coverage on the kinetics of the HOR/HER on Ni. For this purpose, the experimental current-potential curves measured for a freshly polished Ni electrode and for the electrodes oxidized up to various extents were fit by adjusting the rate constants and standard potentials of steps 2 (Heyrovsky), 3 (Volmer), and 4 (surface OH_{ad} formation) using non-linear least squares method. Fitting simultaneously the hydrogen oxidation and evolution reactions (the latter at small overpotentials) is expected to provide a better understanding of the influence of oxide species on the kinetics of Ni electrodes.

Results and Discussion

Electrochemical Properties and Electrocatalytic Activity of Ni in the HOR/HER

Figure 1 presents typical CV curves for a polycrystalline Ni electrode electrochemically oxidized up to various extents. In agreement with the previous findings [14, 19], only one anodic peak (a_1) appears for a freshly polished Ni. Increasing oxidation of the electrode surface (hereinafter, Ni/NiO_x electrodes) leads to a continuous attenuation of peak a_1 and an appearance and growth of additional peaks at lower potentials which are marked as a_2. The detailed discussion about the nature of these two anodic peaks can be found in our previous contributions [14, 19] as well as the studies of other authors [28–30]. Briefly, peak a_1 mostly corresponds to the oxidation of Ni sites with the formation of α-Ni(OH)$_2$, while being partially related to the oxidation of hydrogen adsorbed at potentials below 0 V vs RHE (the latter contribution depends on the negative potential limit of the CV). Peak a_2 is assigned to two processes, namely oxidation of adsorbed hydrogen and the first step of Ni oxidation with the formation of Ni-OH_{ad} (step 5). As discussed below, the position of peak a_2 is mostly determined by the adsorption energy of H_{ad} on Ni surface, which depends on the local oxide coverage. Note that NiO_x
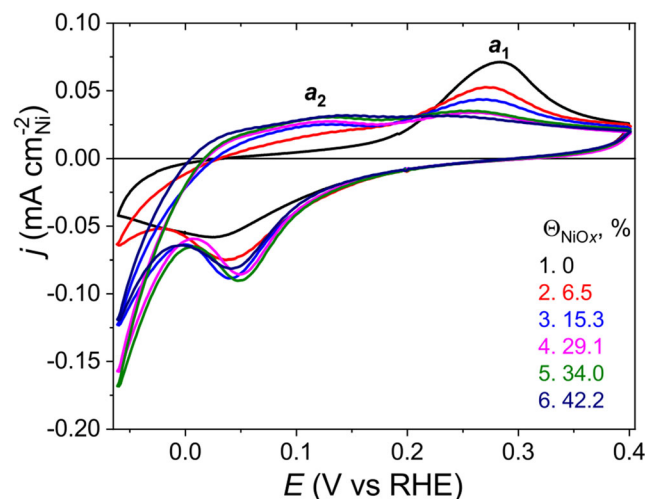
Fig. 1 Cyclic voltammograms of Ni/NiO_x electrodes in Ar-saturated 0.10 M NaOH at $v = 20$ mV s^{-1} and $T = 25$ °C

species formed during electrochemical oxidation at high potentials (Table 1) are stable under the applied conditions because of their ordered structure [31], while the oxides produced during cycling at potentials below 0.40 V (mainly in the form of α-Ni(OH)$_2$) can be reduced by cathodic treatment even at potentials close to 0 V.

The CV curves registered in the presence of hydrogen further support very strong influence of the amount of NiO$_x$ species present on the surface of Ni/NiO$_x$ electrodes on the kinetics of the HOR and the HER (Fig. 2a, b). From these curves, one may clearly see that the anodic peak of hydrogen oxidation shifts from *ca.* 0.25 V (for metallic Ni) towards more negative values with the increase of the NiO$_x$ coverage. The specific activity of the Ni/NiO$_x$ electrodes calculated from micropolarization region of Fig. 2 a and b shows a volcano-type dependence on the NiO$_x$ coverage with a maximum at approximately 30% coverage. The activity increases by a factor of 14 or 12 when normalized by either the ECSA of the available metal Ni sites (Fig. 2c) or by the geometric surface area of the electrode (Fig. 2d), respectively. Interestingly, the exchange current densities slightly differ depending on the cathodic limit of CVs either at − 0.20 or − 0.06 V (Fig. 2c, d). This is likely related to the difference in the surface

state of Ni/NiO$_x$ electrodes in these two cases. Indeed, cycling down to more negative potentials should reduce the electrode surface up to a larger extent as well as produce some amount of Ni hydrides which are believed to have negative effect on the HOR/HER activity of Ni electrodes [32, 33]. Analysis of the CV curves presented on Fig. 2 a and b also shows that the Ni/NiO$_x$ sample with the highest (42%) coverage of oxide species on the electrode surface has poor activity in the HOR, while still showing reasonable performance in the HER. This is likely due to insufficient amount of Ni^0 sites available for the HOR, the latter being rapidly blocked by adsorbed OH$_{ad}$ species at potentials slightly above 0 V vs RHE. Meanwhile, in the HER potential interval, OH$_{ad}$ should not compete with the H$_{ad}$ adsorption especially at high cathodic potentials.

In order to further examine the influence of the NiO$_x$ coverage on the kinetics of the HOR, we performed chronoamperometric measurements at various applied potentials (25, 50, and 100 mV), which are presented in Fig. 3. Corresponding transients show similar descending behavior for all Ni/NiO$_x$ samples with reaching quasi-steady-state values after the initial fast decay. Notably, the current densities normalized by ECSA (Fig. 3a) show similar to the exchange
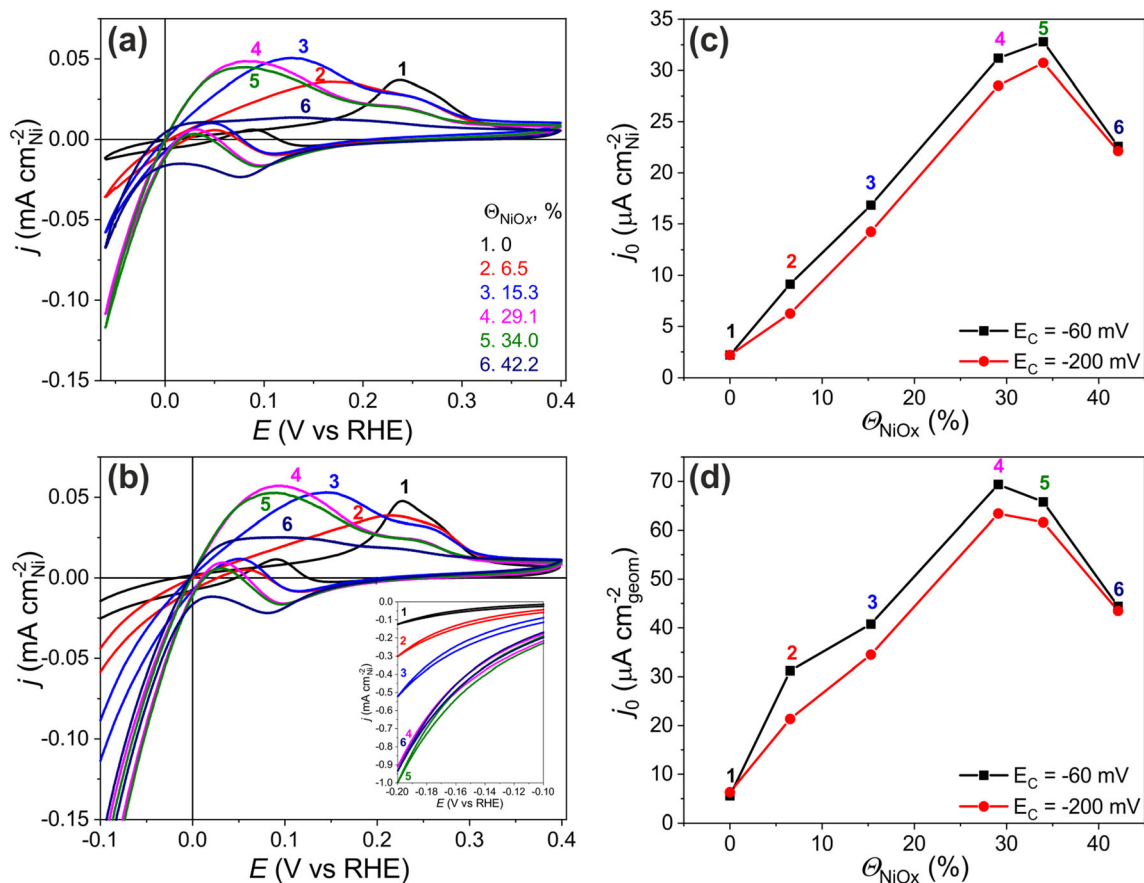
Fig. 2 Cyclic voltammograms of Ni/NiO$_x$ electrodes in H$_2$-saturated 0.10 M NaOH in the potential interval of **a** − 0.06–0.40 V and **b** − 0.2–0.40 V at v = 5 mV s$^{−1}$ and T = 25 °C; Dependence of the exchange current density normalized by either **c** ECSA or **d** geometric surface area of Ni/NiO$_x$ electrodes on the NiO$_x$ coverage
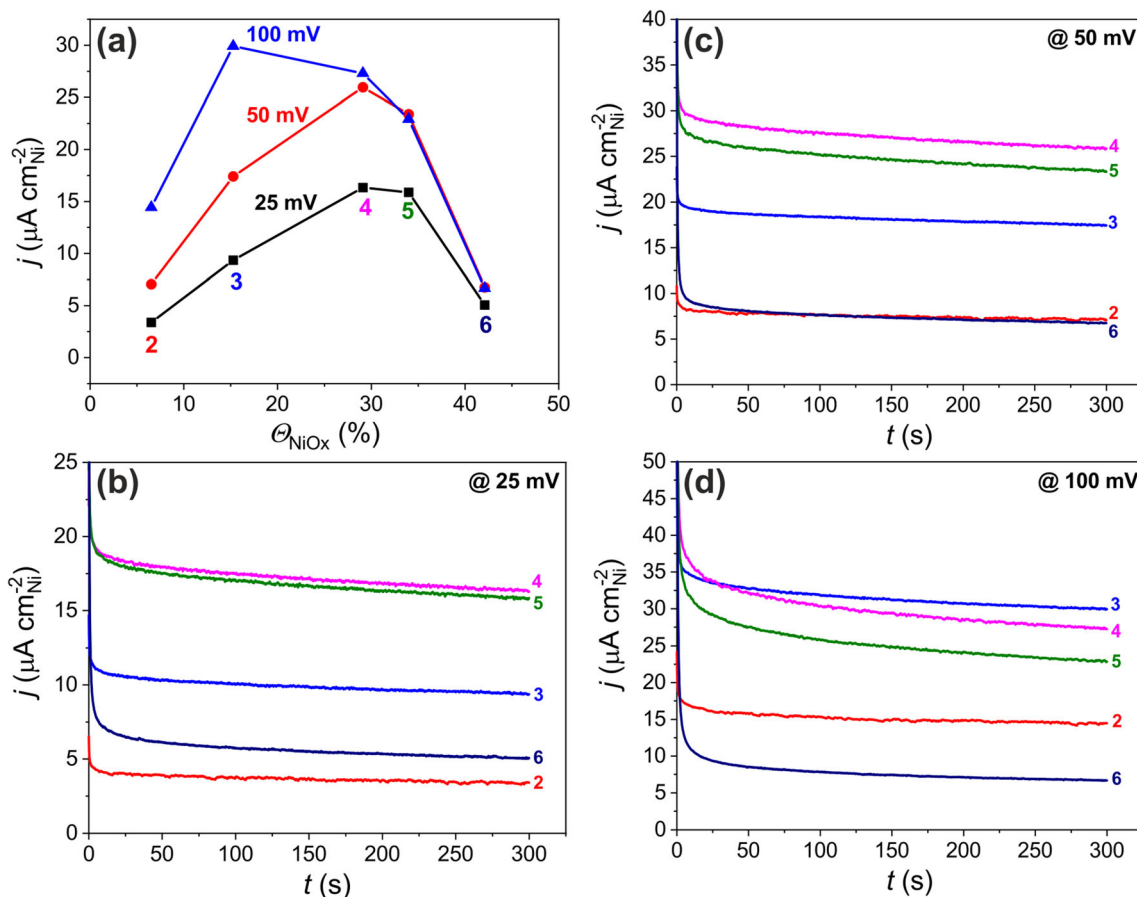
Fig. 3 **a** Dependence of the HOR current densities of Ni/NiO$_x$ electrodes measured at various potentials on the amount of NiO$_x$ at the electrode surface. **b–d** Corresponding transients registered in H$_2$-saturated 0.10 M NaOH at T = 25 °C

current density (Fig. 2c) volcano dependence on the extent of oxidation of Ni/NiO$_x$ electrodes with a maximum at *ca.* 30% coverage by NiO$_x$ species if measured at E = 25 and 50 mV, while at E = 100 mV, higher values were registered with lower NiO$_x$ coverage of *ca.* 15%. Such a difference is likely related to stronger passivation of the surface of Ni/NiO$_x$ electrodes with higher than 15% NiO$_x$ coverage at E = 100 mV. Indeed, as one may see from Fig. 2 a and b, this potential lies on the descending branch of the anodic peak a_2 for Ni/NiO$_x$ samples with 29.1 and 34.0% of NiO$_x$ on the electrode surface. On the contrary, the maximum of the anodic peak a_2 is located above 100 mV for the Ni/NiO$_x$ samples with 15% surface coverage by NiO$_x$ species. The effect of the surface passivation for NiO$_x$ coverages exceeding 15% is further evidenced by the comparison of transients presented on Fig. 3d. Even if the initial values of current densities for samples 4 and 5 are higher than those observed for the sample 3, they are decaying much faster without reaching steady state even after 300 s.

To further explore the influence of the NiO$_x$ concentration on the kinetics of the HER at overpotentials below 200 mV, we analyzed the anodic scans of the CV curves plotted in Tafel coordinates (Fig. 4a). On metallic Ni, the apparent Tafel slope of the HER branch ($-0.20 < \eta < -0.07$ V) amounts to 117

mV/decade being in agreement with the previous findings [19, 34, 35]. At the same time the Tafel slope of partially oxidized Ni/NiO$_x$ electrodes is larger with a maximum value of 142 mV/decade obtained at 29.1% coverage by NiO$_x$ species (Table 1). The high value of the apparent Tafel slope suggests that the Volmer step is rate determining [36, 37]. The exchange current densities extracted from the analysis of the Tafel plots and normalized by either ECSA or geometric surface area of the Ni/NiO$_x$ electrodes are in a good agreement with the data presented on Fig. 2c and d. Similarly, the highest activity values are obtained for the Ni/NiO$_x$ samples with the NiO$_x$ coverage close to 30%, while much higher value (compared with the one determined from the analysis of the micropolarization region) is observed for the strongly oxidized Ni/NiO$_x$ electrode due to the above discussed reasons.

Kinetics of the HOR/HER and its Dependence on the Degree of Ni Oxidation

In our previous studies, positive influence of the partial oxidation of Ni electrodes on the HOR/HER activity as well as the shape of CV curves were assigned to an increase of the free energy of the adsorbed hydrogen intermediate and an
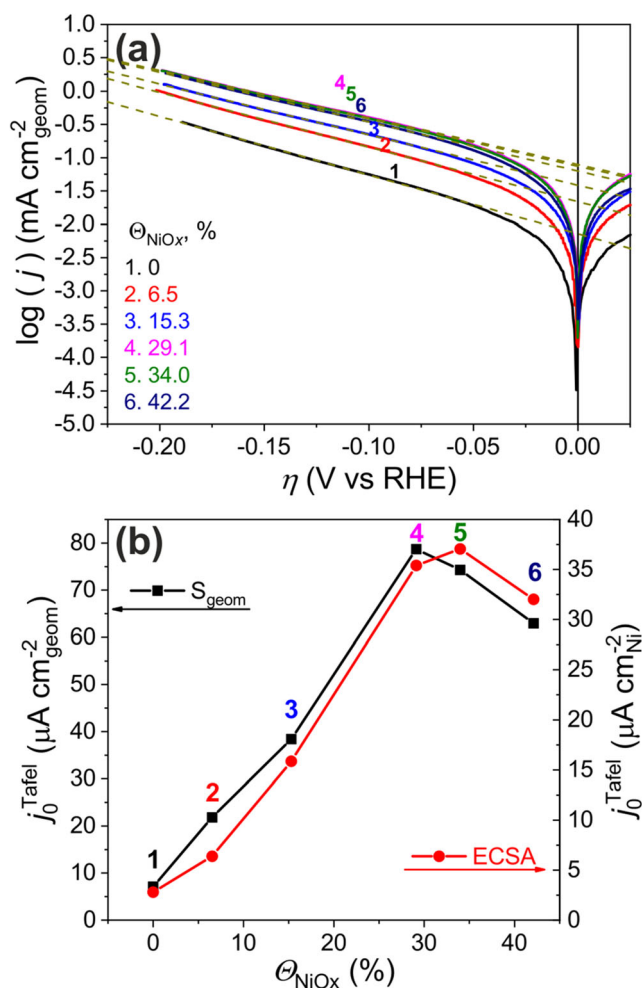
Fig. 4 **a** Tafel plots obtained by plotting anodic scans of CV curves for Ni/NiO$_x$ electrodes in H$_2$-saturated 0.10 M NaOH at $v = 5$ mV s^{-1} and $T = 25$. **b** Dependence of the exchange current density estimated from the corresponding Tafel plots on the amount of NiO$_x$ at the electrode surface

enhanced kinetics of the Volmer step [14, 19]. The main purpose of this study is to verify consistency of the kinetic model with a larger set of data and extract information on the NiO$_x$ coverage dependence of the kinetic parameters. The key results of this study are summarized in Fig. 5. We also analyzed possible effect of the recombination step (7) (see Fig. 6 and the discussion below).

A reasonable agreement between the experimental and simulated current-potential curves was obtained assuming two types of Ni^0 sites on the surface of various Ni/NiO$_x$ electrodes (Fig. 5a, b). The sites of the first type (marked as I) are located at a sufficient distance from surface NiO$_x$ oxides (if present), and give rise to peak a_1, which is present in all CV curves. The second type of sites corresponds to the ones situated in the vicinity of surface oxides (which are believed to grow as small islands [38, 39]), giving rise to peak a_2. These sites are marked as II, III, and IV, depending on the number of closely located oxide species and/or their proximity (Fig. 5c).

It should be stressed that all of the sites, I–IV assumed in the kinetic model correspond only to the Ni^0 sites free from NiO$_x$ based on the fact that the latter themselves do not show any activity in the HOR (Figure S2). In this regard, the relative contribution of either of Ni active sites labeled from I to IV is not directly related to the concentration of NiO$_x$ species at the surface of Ni/NiO$_x$ electrodes. Meanwhile, the percentage of the Ni^0 active sites affected by oxide species increases with an increase of the NiO$_x$ coverage (Fig. 5d). Here, we roughly estimate the ratio between the two types of Ni^0 active sites (I and II, I and III, I and IV for Ni/NiO$_x$ samples 2, 3, and 4, respectively) from the experimental current-potential curves as a ratio between the maximum current densities of the corresponding a_1 and a_2 peaks. An actual Ni/NiO$_x$ electrode surface likely comprises a distribution of active sites with different characteristics, the measured current-potential curve resulting from their superposition. The use of in situ microscopic and spectroscopic methods for characterization of the sample structure and composition should reveal real distribution of various Ni sites over the electrode surface. Meanwhile, application of ex situ methods for this purpose is hardly beneficial as the surface state of Ni electrodes strongly depends on the environment in which it is studied.

Notwithstanding the above mentioned complexity, the analysis of the experimental CV curves performed with the help of microkinetic modeling allows drawing several important conclusions. In agreement with the previous findings [14, 19], the value of $\Delta_{ad}G_H^0$ on a freshly polished Ni electrode was estimated as -0.13 eV evidencing too strong adsorption of H$_{ad}$ intermediates, which is responsible for its low HOR/HER performance. Enhancement of the activity on partially oxidized Ni/NiO$_x$ electrodes can be explained by weakening of the strength of H$_{ad}$ adsorption in the vicinity of surface Ni oxides and the corresponding increase of the $\Delta_{ad}G_H^0$ value up to -0.02 eV, which was calculated for the most active surface sites (Fig. 5e). Such a tendency is being generally in agreement with Dong et al. [22]. The change of the $\Delta_{ad}G_H^0$ entails changes in the rates of the Heyrovsky and Volmer steps through the exponential term in Eqs. 8 and 9 (regarding the link between E_V, E_H, and $\Delta_{ad}G_H^0$ the readers are referred to Eqs. 13 and 14). Besides, to reproduce the experimental data, we had to assume a steady increase of the Volmer rate constant k_V^0 with the increase of the NiO$_x$ coverage. Thus, k_V^0 for the most active Ni/NiO$_x$ sample appeared to be 10 times higher compared with the non-oxidized one (Fig. 5f, Table 2). At the same time, the Heyrovsky rate constant k_H^0 was barely affected by the presence of surface oxides, in all increasing by a factor of ca. 3 (Table 2). Note that although the parameters for the formation of Ni-OH$_{ad}$ and Ni-(OH)$_{2,ad}$ were mostly estimated from the analysis of experimental CV curves registered under inert atmosphere (the reader is addressed to our previous works [14, 19] for further details), to be in agreement with the experimental data, it was necessary to take into consideration variation of the potential of the Ni-
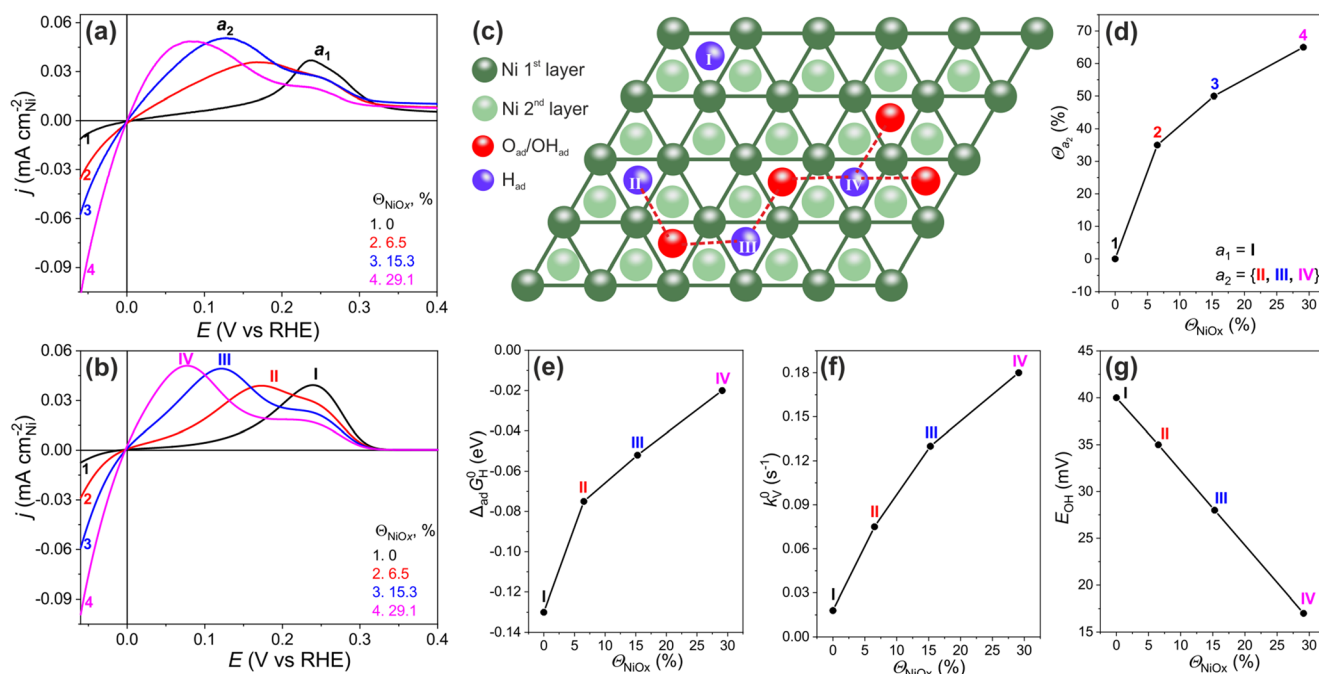
Fig. 5 Comparison of the anodic scans of **a** experimental and **b** simulated CV curves for various Ni/NiO$_x$ electrodes in H$_2$-saturated 0.10 M NaOH at $v = 5$ mV s^{-1} and various degree of oxidation of their surface. **c** Schematic illustration of the Ni active sites with various adsorption energies depending on the number of closely located oxide species. Influence of the NiO$_x$ coverage on **d** the percentage of Ni active sites affected by oxygen species (peak a_2), **e** the free energy of the adsorbed H$_{ad}$ intermediate, **f** the Volmer rate constant k_V^0, and **g** the potential of Ni-OH$_{ad}$ formation

OH$_{ad}$ formation. The latter is decreasing at higher coverage of the electrode surface by stable NiO$_x$ species (Fig. 5 g).
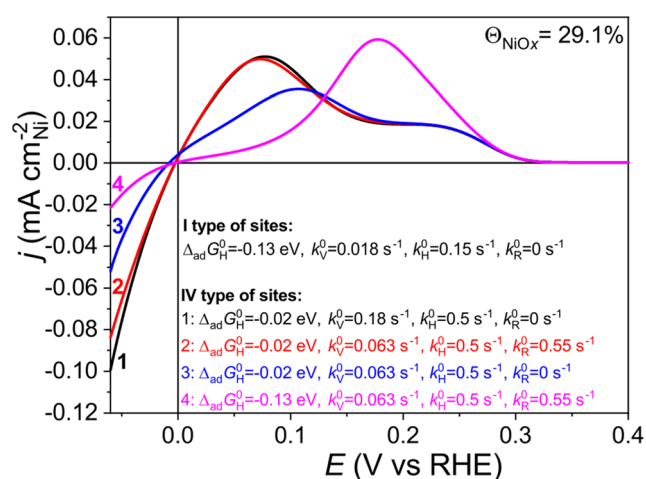
The results of simulations presented in Fig. 5 were obtained disregarding the recombination step (7). Then, simulations were performed by including this step in the model to check its possible influence on the HOR/HER kinetics. The rate of the recombination step can be expressed as:

Fig. 6 Comparison of the anodic scans of simulated CV curves for the Ni/NiO$_x$ electrode with 29.1% of NiO$_x$ coverage in H$_2$ atmosphere at pH = 13 and $v = 5$ mV s^{-1}. The modified parameters for the IV type of Ni^0 sites are listed on the figure, while the other can be found in Table 2

$$v_{R,i} = k_{R,i}^0 \left[\theta_{OH} \cdot \theta_H - \left(1 - \theta_H - \theta_{OH} - \theta_{(OH)_2}\right)^2 \exp\left(\frac{F\left(-E_{OH,i} - E_{V,i}\right)}{RT}\right) \right]$$
(15)

The total Faradaic current density expressed by the Eq. 12 should be then given by:

$$j_F = F \sum_{i=a_1,a_2} \theta_i \left(v_{H,i} + v_{V,i} + v_{OH,i} + v_{(OH)_2,i} + v_{R,i}\right)$$ (16)

If $\Delta_{ad}G_H^0$ was kept constant and equal to the value characteristic of metallic Ni ($\Delta_{ad}G_H^0 = -0.13$ eV), including the recombination step failed to reproduce the experimental data for the Ni/NiO$_x$ electrode with 29.1% of NiO$_x$ coverage (curve 4 in Fig. 6). This emphasizes the importance of the adsorption energy of H$_{ad}$ intermediates for the HOR/HER kinetics and confirms that its decrease with the NiO$_x$ coverage is the key factor determining higher activity of partially oxidized compared with metallic Ni electrodes. Note however that once the absolute value of $\Delta_{ad}G_H^0$ is decreased, contribution of the recombination step in the reaction mechanism cannot be excluded. Indeed, Fig. 6 shows that assuming $\Delta_{ad}G_H^0 = -0.02$ eV, one can reproduce the experimental current-potential curve (see the curve 4 in Fig. 5a), with similar accuracy either by considering high $k_V^0 = 0.18$ s^{-1} and neglecting the recombination step ($k_R^0 = 0$ s^{-1}, curve 1 in Fig. 6), or, alternatively, considering smaller $k_V^0 = 0.063$ s^{-1} but including the recombination step ($k_R^0 = 0.55$ s^{-1}, curve 2 in Fig. 6). This confirms

Table 2 Rate constants for various Ni^0 active sites on the surface of Ni/NiO_x electrodes calculated by fitting the experimental data with the kinetic model

Parameter	Meaning	Peak a_1	Peak a_2		
		Sites I	Sites II	Sites III	Sites IV
k_V^0, s^{-1}	Volmer rate constant	0.018	0.075	0.13	0.18
E_V, V	Volmer standard potential	0.13	0.075	0.052	0.02
k_H^0, s^{-1}	Heyrovsky rate constant	150	500	500	500
E_H, V	Heyrovsky standard potential	-0.49	-0.44	-0.42	-0.38
k_{OH}^0, s^{-1}	OH_{ad} rate constant	100	100	100	100
E_{OH}, V	OH_{ad} standard potential	0.04	0.035	0.028	0.017
$k_{(OH)2}^0$, s^{-1}	$(OH)_{2,ad}$ rate constant	0.1	0.1	0.1	0.1
$E_{(OH)2}$, V	$(OH)_{2,ad}$ standard potential	0.16	0.16	0.16	0.16

that microkinetic modeling cannot unambiguously distinguish between the contribution of these two factors when $\Delta_{ad}G_H^0$ is close to 0 eV.

Conclusions

The kinetics of the hydrogen oxidation and evolution reactions at polycrystalline Ni electrodes oxidized up to different extents was studied. Comparative experiments were performed using cyclic voltammetry and chronoamperometry techniques, which revealed significant variations in the specific activities of Ni/NiO_x electrodes in the HOR/HER with a maximum reached at *ca.* 30% coverage of the Ni surface by NiO_x oxide species. Our results provide experimental evidence for recent theoretical calculations [22], suggesting that the HOR/HER kinetics on Ni active sites is significantly affected by the number of oxygen species located in their vicinity. By combining electrochemical methods with mean-field microkinetic modeling, we conclude, in agreement with the previous findings [14, 19], that the HOR/HER activity of Ni/NiO_x electrodes is mostly determined by the strength of adsorption of H_{ad} intermediates as well as the kinetics of the Volmer step. To explain the experimental observations, one must consider the NiO_x coverage–dependent strength of adsorption of hydrogen atoms, which entails changes in the rates of the Heyrovsky and Volmer steps. In addition to those changes resulting from the exponential term, there seem to be additional changes in the k_V^0 and k_H^0, whose physical reason is currently not fully understood. They could either be due to the double layer effects or due to the interference of the recombination step. It should be emphasized that the recombination step alone (that is without assuming a $\Delta_{ad}G_H^0$ change) cannot explain the experimental observations. Finally, we infer that not only the H_{ad} but also OH_{ad} adsorption strength is affected by the presence of surface NiO_x oxide species.

References

1. Y. Cong, B. Yi, Y. Song, Hydrogen oxidation reaction in alkaline media: from mechanism to recent electrocatalysts. Nano Energy **44**, 288–303 (2018)
2. E.S. Davydova, S. Mukerjee, F. Jaouen, D.R. Dekel, Electrocatalysts for hydrogen oxidation reaction in alkaline electrolytes. ACS Catal. **8**, 6665–6690 (2018)
3. C.A. Campos-Roldán, N. Alonso-Vante, The hydrogen oxidation reaction in alkaline medium: an overview. Electrochem. Energy Rev. **2**, 312–331 (2019)
4. N. Mahmood, Y. Yao, J.-W. Zhang, L. Pan, X. Zhang, J.-J. Zou, Electrocatalysts for hydrogen evolution in alkaline electrolytes: mechanisms, challenges, and prospective solutions. Adv. Sci. **5**, 1700464 (2018)
5. S.A. Kabir, K. Lemire, K. Artyushkova, A. Roy, M. Odgaard, D. Schlueter, A. Oshchepkov, A. Bonnefont, E. Savinova, D. Sabarirajan, P. Mandal, E. Crumlin, I.V. Zenyuk, P. Atanassov, A. Serov, Platinum group metal-free nimo hydrogen oxidation catalysts: high performance and durability in alkaline exchange membrane fuel cells. J. Mater. Chem. A **5**, 24433–24443 (2017)
6. A.G. Oshchepkov, P.A. Simonov, O.V. Cherstiouk, R.R. Nazmutdinov, D.V. Glukhov, V.I. Zaikovskii, T.Y. Kardash, R.I. Kvon, A. Bonnefont, A.N. Simonov, V.N. Parmon, E.R. Savinova, On the effect of cu on the activity of carbon supported Ni nanoparticles for hydrogen electrode reactions in alkaline medium. Top. Catal. **58**, 1181–1192 (2015)
7. O.V. Cherstiouk, P.A. Simonov, A.G. Oshchepkov, V.I. Zaikovskii, T.Y. Kardash, A. Bonnefont, V.N. Parmon, E.R. Savinova, Electrocatalysis of the hydrogen oxidation reaction on carbon-supported bimetallic NiCu particles prepared by an improved wet chemical synthesis. J. Electroanal. Chem. **783**, 146–151 (2016)
8. M.K. Bates, Q. Jia, N. Ramaswamy, R.J. Allen, S. Mukerjee, Composite Ni/NiO-Cr2O3 Catalyst for alkaline hydrogen evolution reaction. J. Phys. Chem. C **119**, 5467–5477 (2015)
9. F. Song, W. Li, J. Yang, G. Han, P. Liao, Y. Sun, Interfacing nickel nitride and nickel boosts both electrocatalytic hydrogen evolution and oxidation reactions. Nat. Commun. **9**, 4531 (2018)

10. W. Ni, A. Krammer, C.S. Hsu, H.M. Chen, A. Schüler, X. Hu, Ni$_3$N as an active hydrogen oxidation reaction catalyst in alkaline medium. Angew. Chem. Int. Ed. **58**, 7445–7449 (2019)

11. M. Gong, W. Zhou, M.J. Kenney, R. Kapusta, S. Cowley, Y. Wu, B. Lu, M.-C. Lin, D.-Y. Wang, J. Yang, B.-J. Hwang, H. Dai, Blending Cr$_2$O$_3$ into a NiO-Ni electrocatalyst for sustained water splitting. Angew. Chem. **127**, 12157–12161 (2015)

12. G. Wang, W. Li, B. Huang, L. Xiao, J. Lu, L. Zhuang, Exploring the composition–activity relation of Ni–Cu binary alloy electrocatalysts for hydrogen oxidation reaction in alkaline media. ACS Appl. Energy Mater. **2**, 3160–3165 (2019)

13. E. Davydova, J. Zaffran, K. Dhaka, M. Toroker, D. Dekel, Hydrogen oxidation on Ni-based electrocatalysts: The Effect of Metal Doping. Catalysts **8**, 454 (2018)

14. A.G. Oshchepkov, A. Bonnefont, V.A. Saveleva, V. Papaefthimiou, S. Zafeiratos, S.N. Pronkin, V.N. Parmon, E.R. Savinova, Exploring the influence of the nickel oxide species on the kinetics of hydrogen electrode reactions in alkaline media. Top. Catal. **59**, 1319–1331 (2016)

15. A.G. Oshchepkov, A. Bonnefont, S.N. Pronkin, O.V. Cherstiouk, C. Ulhaq-Bouillet, V. Papaefthimiou, V.N. Parmon, E.R. Savinova, Nanostructured nickel nanoparticles supported on vulcan carbon as a highly active catalyst for the hydrogen oxidation reaction in alkaline media. J. Power Sources **402**, 447–452 (2018)

16. M. Gong, W. Zhou, M.C. Tsai, J. Zhou, M. Guan, M.C. Lin, B. Zhang, Y. Hu, D.Y. Wang, J. Yang, S.J. Pennycook, B.J. Hwang, H. Dai, Nanoscale nickel oxide/nickel heterostructures for active hydrogen evolution electrocatalysis. Nat. Commun. **5**, 1–6 (2014)

17. X. Liu, X. Wang, X. Yuan, W. Dong, F. Huang, Rational composition and structural design of in situ grown nickel-based electrocatalysts for efficient water electrolysis. J. Mater. Chem. A **4**, 167–172 (2016)

18. J. Wang, S. Mao, Z. Liu, Z. Wei, H. Wang, Y. Chen, Y. Wang, Dominating Role of Ni^0 on the interface of Ni/NiO for enhanced hydrogen evolution reaction. ACS Appl. Mater. Interfaces **9**, 7139–7147 (2017)

19. A.G. Oshchepkov, A. Bonnefont, V.N. Parmon, E.R. Savinova, On the effect of temperature and surface oxidation on the kinetics of hydrogen electrode reactions on nickel in alkaline media. Electrochim. Acta **269**, 111–118 (2018)

20. T. Zhang, M.Y. Wu, D.Y. Yan, J. Mao, H. Liu, W. Bin Hu, X.W. Du, T. Ling, S.Z. Qiao, Engineering oxygen vacancy on NiO nanorod arrays for alkaline hydrogen evolution. Nano Energy **43**, 103–109 (2018)

21. N. Danilovic, R. Subbaraman, D. Strmcnik, K.C. Chang, A.P. Paulikas, V.R. Stamenkovic, N.M. Markovic, Enhancing the alkaline hydrogen evolution reaction activity through the bifunctionality of Ni(OH)$_2$/metal catalysts. Angew. Chem. Int. Ed. **51**, 12495–12498 (2012)

22. Y. Dong, J. Dang, W. Wang, S. Yin, Y. Wang, First-principles determination of active sites of Ni metal-based electrocatalysts for hydrogen evolution reaction. ACS Appl. Mater. Interfaces **10**, 39624–39630 (2018)

23. Y. Pan, G. Hu, J. Lu, L. Xiao, L. Zhuang, Ni(OH)$_2$-Ni/C for hydrogen oxidation reaction in alkaline media. J. Energy Chem. **29**, 111–115 (2019)

24. D. Salmazo, M.F. Juarez, A.G. Oshchepkov, O.V. Cherstiouk, A. Bonnefont, S.A. Shermukhamedov, R.R. Nazmutdinov, W. Schmickler, E.R. Savinova, On the feasibility of bifunctional hydrogen oxidation on Ni and NiCu surfaces. Electrochim. Acta **305**, 452–458 (2019)

25. A. Bonnefont, A.N. Simonov, S.N. Pronkin, E.Y. Gerasimov, P.A. Pyrjaev, V.N. Parmon, E.R. Savinova, Hydrogen electrooxidation on PdAu supported nanoparticles : an experimental RDE and kinetic modeling study. Catal. Today **202**, 70–78 (2013)

26. N. Krstajić, M. Popović, B. Grgur, M. Vojnović, D. Šepa, On the kinetics of the hydrogen evolution reaction on nickel in alkaline solution - Part I. The mechanism. J. Electroanal. Chem. **512**, 16–26 (2001)

27. E.A. Franceschini, G.I. Lacconi, H.R. Corti, Kinetics of the hydrogen evolution on nickel in alkaline solution: New insight from rotating disk electrode and impedance spectroscopy analysis. Electrochim. Acta **159**, 210–218 (2015)

28. M. Alsabet, M. Grden, G. Jerkiewicz, Electrochemical growth of surface oxides on nickel. Part 1: Formation of α-Ni(OH)$_2$ in relation to the polarization potential, polarization time, and temperature. Electrocatalysis **2**, 317–330 (2011)

29. D. Floner, C. Lamy, J.-M. Leger, Electrocatalytic oxidation of hydrogen on polycrystal and single-crystal nickel electrodes. Surf. Sci. **234**, 87–97 (1990)

30. J.L. Weininger, M.W. Breiter, Hydrogen evolution and surface oxidation of nickel electrodes in alkaline solution. J. Electrochem. Soc. **111**, 707–712 (1964)

31. D.S. Hall, D.J. Lockwood, C. Bock, B.R. MacDougall, Nickel hydroxides and related materials: a review of their structures, synthesis and properties. Proc. R. Soc. A Math. Phys. Eng. Sci. **471**, 20140792 (2014)

32. D.M. Soares, Hydride effect on the kinetics of the hydrogen evolution reaction on nickel cathodes in alkaline media. J. Electrochem. Soc. **139**, 98–105 (1992)

33. H.E.G. Rommal, P.J. Morgan, The role of absorbed hydrogen on the voltage-time behavior of nickel cathodes in hydrogen evolution. J. Electrochem. Soc. **135**, 343–346 (1988)

34. M. Grdeń, G. Jerkiewicz, Influence of surface treatment on the kinetics of the hydrogen evolution reaction on bulk and porous nickel materials. Electrocatalysis. **10**, 173–183 (2019)

35. A. Lasia, A. Rami, Kinetics of hydrogen evolution on nickel electrodes. J. Electroanal. Chem. **294**, 123–141 (1990)

36. B.E. Conway, M. Salomon, Electrochemical reaction orders: applications to the hydrogen- and oxygen-evolution reactions. Electrochim. Acta **9**, 1599–1615 (1964)

37. S. Trasatti, Electrocatalysis of hydrogen evolution : progress in cathode activation, (1992).

38. A. Seghiouer, J. Chevalet, A. Barhoun, F. Lantelme, Electrochemical oxidation of nickel in alkaline solutions: A voltammetric study and modelling, J. Electroanal. Chem. **442**, 113–123 (1998)

39. M. Nakamura, N. Ikemiya, A. Iwasaki, Y. Suzuki, M. Ito, Surface structures at the initial stages in passive film formation on Ni(111) electrodes in acidic electrolytes. J. Electroanal. Chem. **566**, 385–391 (2004)